PCCP

PAPER

View Article Online
View Journal | View Issue

Cite this: *Phys. Chem. Chem. Phys.*, 2019, **21**, 22647

Structural phase transitions in VSe_2: energetics, electronic structure and magnetism†

Georgy V. Pushkarev,[a] Vladimir G. Mazurenko,[a] Vladimir V. Mazurenko[a] and Danil W. Boukhvalov *[ba]

Received 2nd July 2019,
Accepted 20th September 2019

DOI: 10.1039/c9cp03726h

rsc.li/pccp

First principles calculations of the magnetic and electronic properties of VSe_2 describing the transition between two structural phases (H,T) were performed. The results of the calculations evidence a rather low energy barrier (0.60 eV for the monolayer) for the transition between the phases. The energy required for the deviation of a Se atom or whole layer of selenium atoms by a small angle of up to 10° from their initial positions is also rather low, 0.32 and 0.19 eV/Se, respectively. The changes in the band structure of VSe_2 caused by these motions of Se atoms should be taken into account for analysis of the experimental data. Simulations of the strain effects suggest that the experimentally observed T phase of the VSe_2 monolayer is the ground state due to substrate-induced strain. Calculations of the difference in the total energies of the ferromagnetic and antiferromagnetic configurations evidence that the ferromagnetic configuration is the ground state of the system for all stable and intermediate atomic structures. Calculated phonon dispersions suggest a visible influence of the magnetic configurations on the vibrational properties.

1 Introduction

Monolayer VSe_2 is one of the most intriguing members of the family of two-dimensional (2D) transition-metal dichalcogenides. This material has attracted special attention from the scientific community due to several recent discoveries, including in-plane piezoelectricity,[1] a pseudogap with a Fermi arc[2] at temperatures above the charge density wave transition (220 K for the monolayer[3]), and especially the existence of ferromagnetism in the 2D system.[4–11] Experimental results are rather contradictory. Strong room-temperature ferromagnetism with a huge magnetic moment per formula unit has been reported for monolayer VSe_2 epitaxially grown on graphite.[4] A local magnetic phase contrast has also been observed by magnetic force microscopy at room temperature at the edges of VSe_2 flakes exfoliated from a three-dimensional crystal.[12] XMCD measurements evidence a spin-frustrated magnetic structure in VSe_2 on graphite.[13] Paramagnetism of bulk VSe_2[14,15] makes these observations more intriguing. Another situation was reported for monolayers grown on bilayer graphene/silicon carbide substrates. In both studies the absence of exchange splitting of the vanadium 3d bands observed in angle-resolved photoemission spectroscopy experiments was reported. This result contradicts other studies that revealed a magnetization value not higher than 5 μ_B.[16,17] Based on these results we can conclude that the influence of the substrate is important for description of the magnetic properties of these materials. Theoretical models have been developed to account for the above discrepant observations.[4,12,16,18] These studies mainly focused on the band structure and magnetic moments on vanadium sites. It has been proposed that the presence of charge density waves could cause the quenching of monolayer ferromagnetism due to the band gap opening induced by Peierls distortion.[19] Phonon spectra of several VSe_2 and similar systems were also considered theoretically.[20,21] This modeling motivates us to study the interplay between magnetism and structural phase transitions in VSe_2. Additionally, there is a plethora of studies demonstrating a relationship between the symmetry, electronic structure and magnetic properties in transition metal compounds.[22–25]

The VSe_2 crystal is formed from separate layers along the *c*-axis direction. Two main phases for this material were predicted to be stable: the H phase characterized by Se stacked over each other and the T phase with one layer of Se rotated by 60° around the axis normal to the plane of the layer.[18] The atomic structures of the VSe_2 monolayer in both the H and T phases are shown in Fig. 1. Surprisingly, the reported binding energies for different configurations are almost the same despite the colossal difference in magnetic properties and electronic structure (Fig. 1).[18] This finding additionally motivates us to examine various aspects of structural phase transitions in bulk, few-layer and monolayer VSe_2.

[a] *Ural Federal University 620002, 19 Mira Street, Ekaterinburg, Russia. E-mail: contact@urfu.ru; Tel: +7 343 375 4444*
[b] *College of Science, Institute of Materials Physics and Chemistry, Nanjing Forestry University, Nanjing 210037, P. R. China*

† Electronic supplementary information (ESI) available. See DOI: 10.1039/c9cp03726h

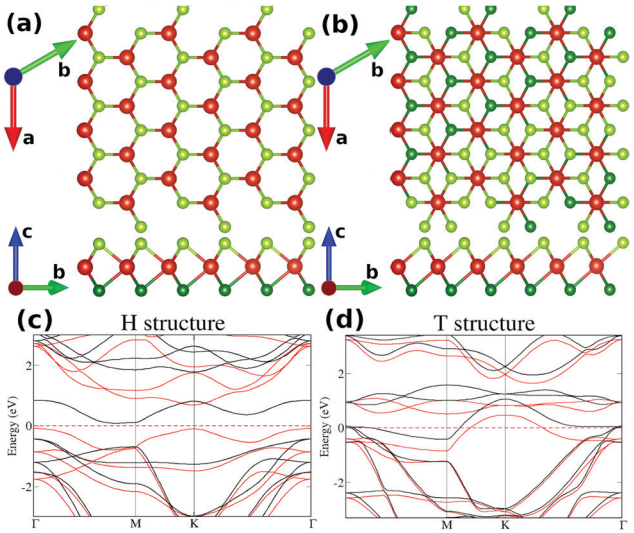

Fig. 1 Atomic structure of the 2D VSe_2 monolayer (top and side view) in the H phase (a) and in the T phase (b). Vanadium atoms are denoted with red circles, and the upper and bottom selenium layers are denoted with light green and dark green circles, respectively. The (c and d) Panels represent the corresponding spin-polarized band structures. The red lines correspond to spin up states and the black ones to spin down, the Fermi level corresponds to 0 eV.

2 Computational method and model

The electronic properties of the VSe_2 system were simulated within the Density Functional Theory (DFT) framework using the Perdew–Burke–Ernzerhof (PBE) exchange–correlation functional[26] as implemented in the Vienna Ab initio Simulation Package (VASP)[27,28] with a plane-wave basis set. This approach gave reliable results for other systems similar to VSe_2.[29] Also we include van der Waals interactions using the method of Grimme (DFT (PBE)-D2).[30] Taking into account London dispersion forces is essential for few-layer VSe_2 (see Table 1 and the discussion in Section 3.5).

The calculation parameters were chosen as follows. The energy cutoff is equal to 400 eV and the energy convergence criterion is 10^{-6} eV. For the Brillouin zone integration a $10 \times 10 \times 1$ gamma centered grid was used for layered structures and $8 \times 8 \times 8$ for bulk structures. A vacuum space of more than 10 Å in the vertical z direction was introduced for layered structures. The technical parameters are similar to those used in the recent studies of phase stability in layered systems.[31,32]

The optimized atomic positions for the T-phase and lattice parameters $a = b = 3.31$ Å and $c = 6.20$ Å are in good agreement with experiment.[33] In particular, the corresponding interlayer distance in bulk VSe_2 is 3.04 Å. The calculated band structures of the VSe_2 monolayer in the T and H phases are in good agreement with previous work.[18] The calculated magnetic moment of 0.68 μ_B for the initial configuration without rotation of the selenium atoms also agrees with the results of previous work.[34]

To investigate the transition between the H and T phases we performed self-consistent calculations of the electronic structure and total energies at the transitional points between these phases. For this purpose, we rotate either one Se atom or all selenium atoms belonging to the upper layer of VSe_2 in the supercell as schematically shown in Fig. 2. To trace the changes in the electronic structure and magnetic properties, calculations for configurations with a 10° rotation step were performed. Generally, the rotation can be realized within two models. The first one is to move one Se atom in plane from the initial to the final point (Fig. 2a and c). The second one is to fix a constant V–Se distance for all intermediate steps, which produces an elevation of selenium atoms above the plane at intermediate steps of the migration (Fig. 2b and d). We will refer to these rotation models as in-plane and arc rotation schemes, respectively. All the calculations were performed for ferromagnetic ordering of the spins of vanadium atoms.

3 Results and discussion

3.1 Rotation of a single Se atom

In the first step of our study we have simulated the motion of a single Se atom in the monolayer (see Fig. 3). For simplicity, we considered in-plane migration of the atom. The results of the calculations (Fig. 3) evidence a gradual increase of the total energy of the system during the whole process of rotation with a maximal value at the final point. The cause of the large magnitude of the energies and instability of the final configuration is the decrease of the distance between the moved and rigid Se atoms to the value of 1.92 Å. Thus we can conclude that the model of single Se atom rotation is unrealistic and the transition between the T and H phases may be realized only with distortion of the whole selenium layer. Further we will consider only this kind of structural phase transitions. The values of the magnetic moments calculated for the intermediate configurations (Fig. 3) support our

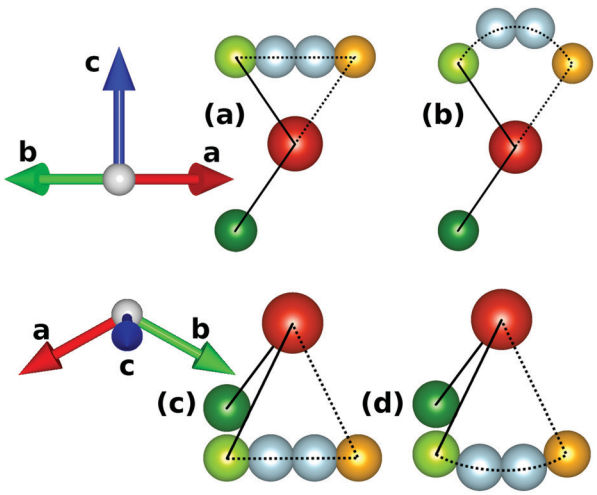

Fig. 2 Schematic visualization of the plane (a and c) and arc (b and d) types of the Se atom rotation. The (a and b) and (c and d) panels correspond to side and top views, respectively. The initial and final positions of Se are presented with orange and green circles, respectively. The intermediate configurations of selenium atoms obtained with a 20° step are denoted with light blue circles.

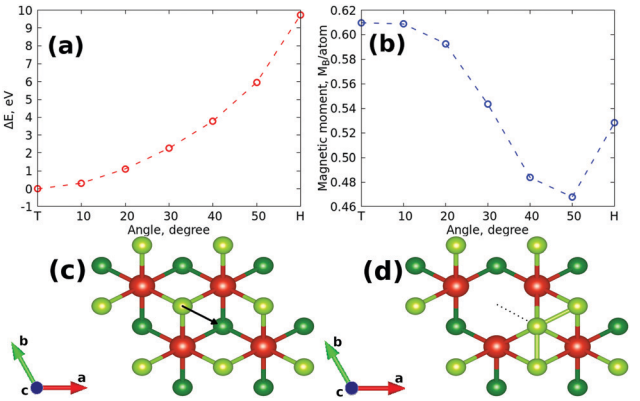

Fig. 3 Evolution of the total energy (a) and magnetic moment (b) during in-plane rotation of a single Se atom. The (c and d) panels visualize the initial and final atomic structures. The light and dark green circles denote the upper and bottom selenium layers, respectively.

initial guess that the structural transition between the phases affects the magnetic properties of VSe_2. Note that a deviation of the selenium atoms from their equilibrium positions by small angles (less than 10°) requires much smaller energies of about 0.32 eV and, therefore, should be taken into account for a realistic description of the atomic structure of VSe_2 at room temperature.

3.2 Rotation of the whole Se sheet in the VSe_2 monolayer

Having considered the results concerning the migration of a single Se atom we are in a position to analyze the case of whole upper Se-layer rotation, which will provide a better understanding of the transition between the H and T phases.

The performed simulations for a 3 × 3 supercell with constant V–Se distances when the Se atoms are elevated from their initial and starting positions (Fig. 2) revealed an energy barrier of 0.60 eV, which is smaller than that observed in the case of the in-plane rotation (Fig. S1a in the ESI†). Thus further we will consider only this type of Se atom migration. To evaluate the temperature required to overcome this barrier one should establish a relation between the calculated energies of the process and the temperature of the reaction. We have addressed this question in our previous work[35] and found that barrier values of about 0.50 eV and 1.20 eV correspond to room temperature and 200 °C, respectively. Thus, the energy barrier of 0.60 eV can be overcome already at temperatures of about 40 °C.

Four conclusions could be drawn from these results. (i) There is a possibility of the structural phase transition in previously studied VSe_2 samples during measurements. (ii) For development of devices based on VSe_2 and similar monolayer systems one should take into account the possibility of structural phase transitions caused by the heating of the devices during operation. Such a transition can significantly affect the functioning of the device due to differences in the electronic structures of different phases (see Fig. 1, also changes in band structure Fig. S3 in the ESI†). (iii) One can use VSe_2 and similar systems as temperature detectors. (iv) According to our results there is a low-energy cost to deviate the selenium atoms belonging to one layer by a small angle from the equilibrium positions. It means that one needs to account for this for a realistic interpretation of the experimental data.

The moderate temperature of the transition between different structural phases requires an examination of the electronic structure and magnetic properties at intermediate steps of the structural phase transition. The obtained calculation results demonstrate that in the case of the ferromagnetic ground state the values of the magnetic moments change gradually with a small step of 10° of the rotation of the Se layer. From Fig. 4 one can see that at 30° the magnetic moment has the maximal value of 1.05 μ_B, which is about two times larger than that in the initial configuration. According to the calculated occupation matrices such a magnetic moment change is mainly related to the contributions of the xy and $x^2 - y^2$ orbitals of vanadium atoms (see Fig. 5). Since the total occupation (spin-up + spin-down) of the different orbitals remains almost the same, the orbital magnetic moment value change is fully connected with a redistribution of the electrons between different spin channels due to change of the hybridization between V and Se.

In the case of an antiferromagnetic configuration the situation is more complicated. First of all, the magnetic lattice of VSe_2 is a frustrated one, which is in agreement with experimental observations.[13] This means that within a mean-field DFT approach we cannot define an antiferromagnetic collinear-type order corresponding to a minimum of the magnetic interaction energy for all V–V bonds, simultaneously. The second complication follows from the fact that the system in question is a metal. It means that the magnetization of individual vanadium atoms can be very sensitive to the orientation of the neighbouring magnetic moments.[36] Indeed, our DFT simulations of the VSe_2 supercell with antiferromagnetic ordering have revealed strong suppression of the magnetic moment values of some vanadium atoms in the supercell. In addition, we observe that the details of the magnetic moment suppression strongly depend on the size of the supercell. In this complex situation some information on magnetic couplings in the VSe_2 system could be extracted by using the theory of infinitesimal spin rotations approximation.[36,37] However, the magnetic couplings calculated in this way can be used for analysis only in the vicinity of the ferromagnetic configuration.

The values of the magnetic moments in the AFM phase can be stabilized by inclusion of the on-site Coulomb interaction as can be done with the DFT+U approach. However, the use of the

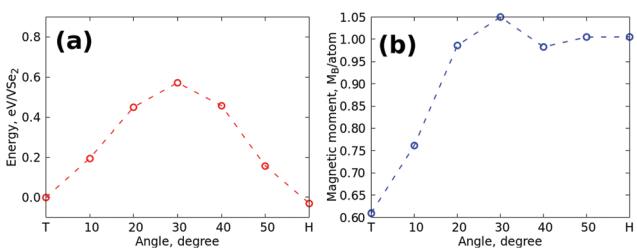

Fig. 4 Evolution of the total energy (a) and magnetic moment (b) during rotation of the whole upper Se layer of the VSe_2 monolayer within the arc model.

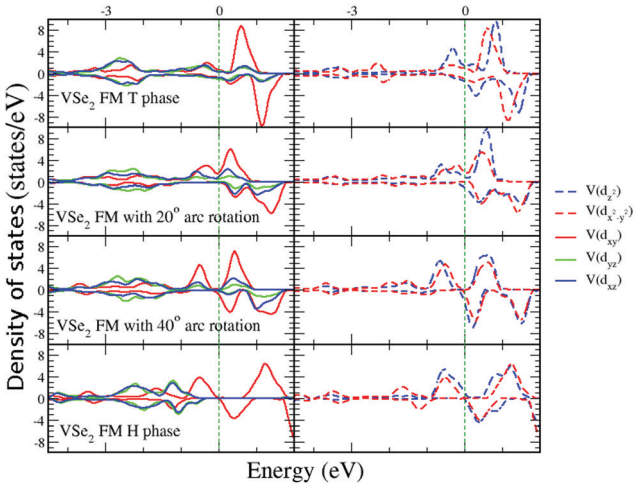

Fig. 5 Partial densities of states calculated for the VSe_2 monolayer in the ferromagnetic configuration. The arc rotation scheme with a 20° step was used. The left and right panels correspond to the (d_{xy}, d_{yz}, d_{xz}) and ($d_{x^2-y^2}$, d_{z^2}) sets of states, respectively.

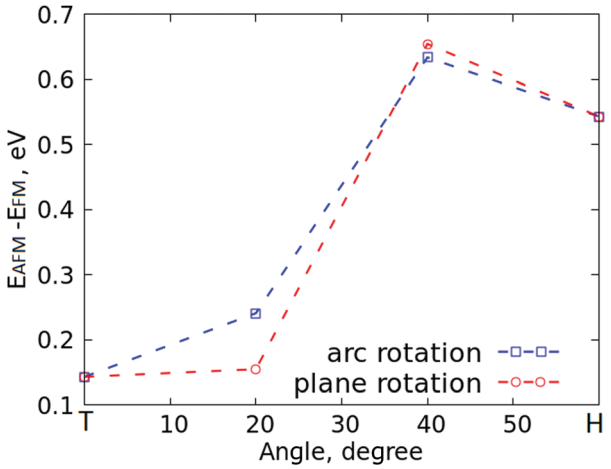

Fig. 6 Difference of AFM and FM state total energies calculated in the arc and plane rotation schemes for a 3 × 3 supercell of the VSe_2 monolayer.

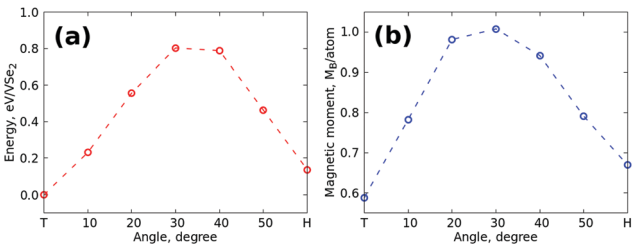

Fig. 7 Total energy (a) and magnetic moment (b) as functions of the rotation angle. The simulation results were obtained for bulk VSe_2 within the arc rotation model.

DFT+U approach in the case of VSe_2 is questionable, since the experimental ARPES spectra are in good agreement with the GGA band structure as it was shown in ref. 13, 16 and 38. At the same time the inclusion of the Hubbard U leads to considerable changes in the band structure.

Thus, the energy difference between the AFM and FM solutions for VSe_2 simulated with GGA does not allow us to construct a comprehensive magnetic model and estimate the corresponding magnetic interactions between vanadium atoms. Nevertheless, the results of these calculations evidence that despite the changes of electronic structure at intermediate steps the ferromagnetic configuration remains significantly energetically favorable in all the cases (Fig. 6). Thus the possible structural distortions in VSe_2 will not provide suppression of ferromagnetism. Our calculations demonstrate that the possible transition from the experimentally observed T phase toward the H phase should provide an enhancement of ferromagnetic interactions and increase of the magnetic moment. To simulate the experimentally observed paramagnetic state of bulk VSe_2[14,15] one can use dynamical mean-field theory.

3.3 Structural phase transition in bulk VSe_2

There are two main differences in the energetics of the structural phase transitions in bulk and monolayer VSe_2. The first one is the similar value for the energies of the motion of the Se layer within both rotation models (Fig. 7 and Fig. S1c in the ESI†). The second one is an increase of the migration barrier (see Fig. 7). Both are related to the van der Waals interactions between the layers in bulk VSe_2. The analysis of the calculated partial density of states in this case leads to similar conclusions to those above (see Fig. S2 in the ESI†).

In the case of the rotation of the Se atoms belonging to one layer with a constant V–Se distance at intermediate steps of migration, the initial distance of 3.63 Å between the rotated and fixed selenium layers decreases by 0.54 Å. This deviation from the optimal interlayer distance provides an increase of the energy barrier (see also changes in the band structure, Fig. S4 in the ESI†). The value of the energy barrier corresponds with the stability of the structural ground state in the bulk crystal up to temperatures above 100 °C. Note that in contrast to the monolayer case the structural ground state of bulk VSe_2 is the T configuration with ferromagnetic orientation of the magnetic moments.

3.4 Structural phase transition in bi- and trilayers of VSe_2

Moreover, we examine the energetics of the structural phases transition in the top layer of bi- and trilayer VSe_2 with different stacking models (Fig. 8). The notation of the types of Bernal stacking is similar to graphite. These results also can be applied for VSe_2 non-covalently attached to substrates.

The results of the calculations (Fig. 9) evidence the similarity of the case of few-layer VSe_2 to the monolayer. The configuration of the H type corresponds to the structural ground state for all types of stacking in the few-layer case. The energy required for the transition from the T to the H phase is about 0.60 eV for AA- and AB-stacking in the bilayer. In the trilayer the most energetically favorable stacking orders are AAA and ABC.

Thus, similarly to the free standing VSe_2 monolayer, in the top layer of VSe_2 there can be a transition between two structural configurations at moderate heating. The magnetic

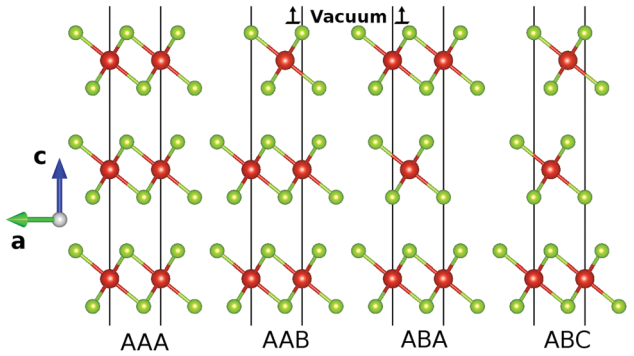

Fig. 8 Schematic representation of the unit cells used for simulating VSe_2 trilayers characterized by different stacking models.

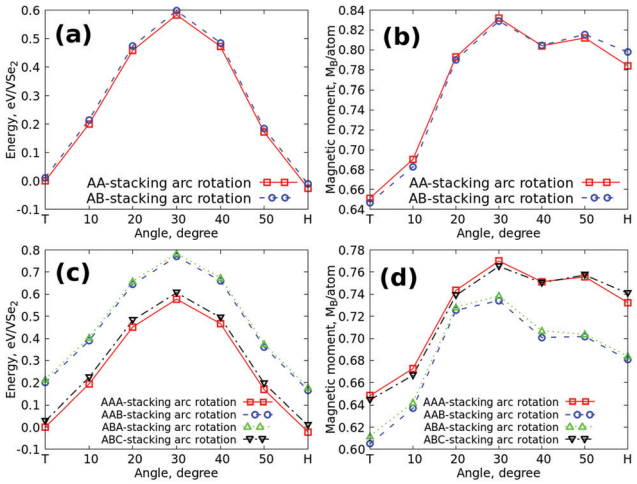

Fig. 9 Total energy (left panels) and magnetic moment (right panels) of two- (a and b) and three-layer (c and d) VSe_2 systems estimated for H, T and intermediate structures.

moments of vanadium atoms belonging to the upper layer of the few-layer structures change from 0.64 μ_B to 0.82 μ_B. Such a change is fully connected with a redistribution of the electrons between different spin channels; the main contributions are from the xy and x^2-y^2 orbitals of vanadium atoms similar to the monolayer case. Therefore, the presence of the substrates does not influence significantly the sensitivity of bi- and trilayer VSe_2 systems to structural changes.

3.5 Interlayer binding energy

To understand the effect of interlayer interactions on the structural properties we have checked the interlayer distances and binding energies. The binding energies E_b for different VSe_2 structures were calculated by using the following expression $E_b = (E - n \times E_{mono})/m$, where E is the total energy of the considered system, E_{mono} – total energy of the monolayer, n – number of layers in the considered system, and m – average number of interlayer interactions (m = 2, 3/2 and 1 for the bulk, and 3 and 2-layers, respectively). The results of these calculations are presented in Table 1.

Table 1 Interlayer binding energies (meV/formula unit) and interlayer distances calculated for different VSe_2 structures with and without vdW interactions

VSe_2 structure	E_b with vdW, meV	E_b without vdW, meV	Interlayer distance with vdW (without vdW), Å
T-bulk	7.93	4.79	3.04 (3.12)
H-bulk	99.67	95.78	3.22 (3.32)
T-two	15.51	−9.36	3.11 (3.51)
H-two	24.68	−29.86	3.69 (4.27)
T-three	19.05	−90.86	3.08 (3.57)
H-three	100.82	−51.77	3.66 (4.14)

In the case where van der Waals interactions are neglected we find that the distance between V–V atoms belonging to the same layer is 3.33 Å and the Se–Se interlayer distance equals 3.12 Å. When the van der Waals interactions are taken into account such distances equal 3.31 Å and 3.04 Å, respectively. In the 2- and 3-layer cases we considered the structures (Fig. 8) with the lowest total energies. The calculated values of the binding energies evidence that few-layer VSe_2 is a pure van der Waals structure in contrast to bulk VSe_2 where London dispersion forces are a small addition to the electrostatic interactions between V-cations and Se-anions from different layers. The changes of interlayer distances are proportional to the contribution of the dispersion forces to the binding energies (about 0.1 Å in the bulk and 0.4–0.6 Å in the few-layer systems). Therefore, the energy difference in the migration barriers in bulk and few-layer VSe_2 can be explained by the contribution from electrostatic repulsion of anions from the layer above.

3.6 Phonon dispersion

To complete the picture of the physical properties of the VSe_2 monolayer we have performed calculations of phonon dispersions by using the VASP and Phonopy packages.[39] This combination of packages is widely used for studying the vibrational properties of similar systems.[31] For such calculations we used a 3 × 3 × 1

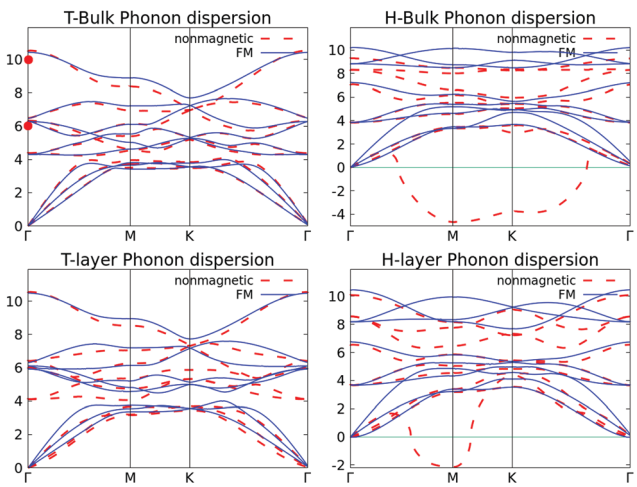

Fig. 10 Phonon dispersions calculated for the nonmagnetic (red dashed line) and the ferromagnetic state (blue solid line) of monolayer and bulk VSe_2. Both T and H phase structures are presented. The red dots denote experimental frequencies taken from ref. 40.

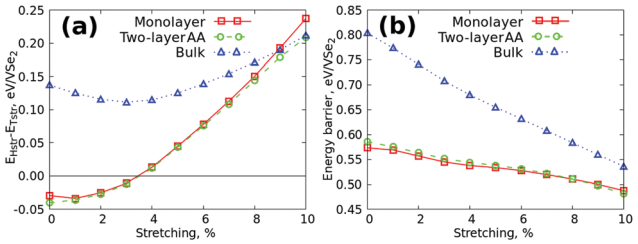

Fig. 11 Energy difference between the H and T structures of VSe_2 (a) and the energy barrier (b) as functions of stretching in the *a* and *b* lattice directions. Lines of different colors correspond to systems with different numbers of layers.

supercell to obtain sets of forces and mesh grids: $10 \times 10 \times 1$ for the monolayer and $6 \times 6 \times 6$ for the bulk. Both the H and T phases in nonmagnetic and ferromagnetic configurations were considered.

The calculated phonon spectra are presented in Fig. 10. For the T phase systems (bulk and monolayer) the resulting dispersions demonstrate a weak sensitivity to the magnetism. It is not the case for the H phase configurations. In the nonmagnetic state for the H-monolayer and H-bulk we observe a soft phonon mode in the direction Γ–M–K for the monolayer and in all symmetry directions for the bulk. The existence of such a mode indicates structural instability. Importantly, in the ferromagnetic case the soft mode disappears, which means that the magnetism provides structural stability of the H phase in both the monolayer and the bulk. The cause of this effect of the magnetic configurations is the robustness of magnetic interactions (see Fig. 6 and the discussion above), which are the same order of magnitude as the difference between structural phases. For the H-bulk and T-monolayer ferromagnetic systems the calculations reveal the appearance of an indirect gap of 0.57 THz. Comparison of the calculated dispersion curves with available experimental data from ref. 40 obtained by point-contact spectroscopy and Raman methods can be fulfilled only for the Γ point for which the experimental oscillation frequencies are 6.04 (25 meV) and 9.67 (40 meV) THz. Our theoretical values of 6.28 and 10.42 THz are in good agreement with the experimental data.

3.7 Structural phase transition by stretching

The last step of our survey is the modeling of stretching, which can appear in the monolayer due to substrate influence. To simulate this effect, we increase the *a* and *b* lattice vectors of our structure and then relax the atomic positions to find a new ground state corresponding to the new lattice parameters. The results of the calculation evidence that stretching of more than 3 percent leads to a phase transition of the ground state configuration from H to T in monolayer and bilayer VSe_2 (Fig. 11a).

Therefore, the experimentally observed structure[13] of the T type can result from substrate-induced strain. Another effect of stretching is a decreasing energy barrier for migration between different configurations (Fig. 11b). Here we define the energy barrier as the energy difference between the T structure and the intermediate 30° structure.

4 Conclusions

The results of first-principles calculations demonstrate that the energy barrier for the transition between two structural states of the VSe_2 monolayer with a step-by-step rotation of a single Se atom is rather high. On the other hand the energy cost of the rotation of a whole selenium layer is rather low (about 0.60 eV for the monolayer and 0.80 eV for the bulk). In the case of the monolayer it could be realized with heating of the samples. The excitation energies of the rotation of the selenium layer up to 10° are very low, therefore, a realistic theoretical description of VSe_2 (from the monolayer to the bulk) should take into account these small deviations from the ideal crystal structure.

Our calculations demonstrate that the transition from the experimentally observed T configuration to the H configuration is accompanied by a considerable change in the electronic structure, which is a redistribution of 3d electrons of vanadium between orbitals. Such transitions significantly influence the transport and thermal properties of VSe_2. On the other hand, the values of the magnetic moments and total energies of the ferro- and antiferromagnetic configurations change gradually between the two structural phases.

In all the considered cases (bulk, few-layer and monolayer) the systems demonstrate strong favorability of the ferromagnetic structure. The analysis of the calculated phonon dispersions has demonstrated a principal role of ferromagnetism in stabilization of the atomic structure of the VSe_2 monolayer in the H phase and similar systems. On the basis of the obtained results we can conclude that the experimentally observed paramagnetism in bulk VSe_2 and contradictory results of magnetic measurements for monolayers on different substrates are not caused by structural changes.

The calculations for bi- and trilayers demonstrate that the energy barrier of the transition is similar to the monolayer. Strain, possibly induced by a substrate, provides the change of the most energetically favorable structure from H to T. Therefore, the experimental observation of the T configuration can result from the VSe_2 structure stretching by more than 3 percent on substrates. Another effect of the stretching is a decrease of the energy barrier of the transition between structural phases. Thus both strain and deviation from the ideal structure should be taken into account for a realistic description of the VSe_2 monolayer on substrates.

Conflicts of interest

There are no conflicts to declare.

Acknowledgements

This work was supported by the Russian Science Foundation, Grant No. 18-12-00185.

Notes and references

1 J. Yang, A. Wang, S. Zhang, J. Liu, Z. Zhong and L. Chen, *Phys. Chem. Chem. Phys.*, 2019, **21**, 132–136.
2 Y. Umemoto, K. Sugawara, Y. Nakata, T. Takahashi and T. Sato, *Nano Res.*, 2019, **12**, 165–169.

3 P. Chen, W. Pai, Y. Chan, V. Madhavan, M. Chou, S. Mo, A. Fedorov and T. Chiang, *Phys. Rev. Lett.*, 2018, **121**, 196402.
4 M. Bonilla, S. Kolekar, Y. Ma, H. Coy Diaz, V. Kalappattil, R. Das, T. Eggers, H. Rodriguez Gutierrez, M.-H. Phan and M. Batzill, *Nat. Nanotechnol.*, 2018, **13**, 289–293.
5 Q. Wu, Y. Zhang, Q. Zhou, J. Wang and X. C. Zeng, *J. Phys. Chem. Lett.*, 2018, **9**, 4260–4266.
6 Z. Wang, T. Zhang, M. Ding, B. Dong, Y. Li, M.-L. Chen, X. Li, J.-Q. Huang, H. Wang, X. Zhao, Y. Li, D. Li, C. Jia, L. Sun, H. Guo, Y. Ye, D. Sun, Y. Chen, T. Yang and Z. Zhang, *Nat. Nanotechnol.*, 2018, **13**, 554–559.
7 D. J. O'Hara, T. Zhu, A. H. Trout, A. S. Ahmed, Y. K. Luo, C. H. Lee, M. R. Brenner, S. Rajan, J. A. Gupta, D. W. McComb and R. K. Kawakami, *Nano Lett.*, 2018, **18**, 3125–3131.
8 S. Jiang, L. Li, Z. Wang, K. F. Mak and J. J. Shan, *Nat. Nanotechnol.*, 2018, **13**, 549–553.
9 N. C. Frey, H. Kumar, B. Anasori, Y. Gogotsi and V. B. Shenoy, *ACS Nano*, 2018, **12**, 6319–6325.
10 D. V. Averyanov, I. S. Sokolov, A. M. Tokmachev, O. E. Parfenov, I. A. Karateev, A. N. Taldenkov and V. G. Storchak, *ACS Appl. Mater. Interfaces*, 2018, **10**, 20767–20774.
11 N. Samarth, *Nature*, 2017, **546**, 216–218.
12 S. Lee, J. Kim, Y. C. Park and S.-H. Chun, *Nanoscale*, 2019, **11**, 431–436.
13 P. K. J. Wong, W. Zhang, F. Bussolotti, X. Yin, T. S. Herng, L. Zhang, Y. L. Huang, G. Vinai, S. Krishnamurthi, D. W. Bukhvalov, Y. J. Zheng, R. Chua, A. T. N'Diaye, S. A. Morton, C.-Y. Yang, K.-H. Ou Yang, P. Torelli, W. Chen, K. E. J. Goh, J. Ding, M.-T. Lin, G. Brocks, M. P. de Jong, A. H. Castro Neto and A. T. S. Wee, *Adv. Mater.*, 2019, **0**, 1901185.
14 C. van Bruggen and C. Haas, *Solid State Commun.*, 1976, **20**, 251–254.
15 M. Bayard and M. Sienko, *J. Solid State Chem.*, 1976, **19**, 325–329.
16 J. Feng, D. Biswas, A. Rajan, M. D. Watson, F. Mazzola, O. J. Clark, K. Underwood, I. Markovic, M. McLaren, A. Hunter, D. M. Burn, L. B. Duffy, S. Barua, G. Balakrishnan, F. Bertran, P. Le Fevre, T. K. Kim, G. van der Laan, T. Hesjedal, P. Wahl and P. D. C. King, *Nano Lett.*, 2018, **18**, 4493–4499.
17 G. Duvjir, B. K. Choi, I. Jang, S. Ulstrup, S. Kang, T. Thi Ly, S. Kim, Y. H. Choi, C. Jozwiak, A. Bostwick, E. Rotenberg, J.-G. Park, R. Sankar, K.-S. Kim, J. Kim and Y. J. Chang, *Nano Lett.*, 2018, **18**, 5432–5438.
18 F. Li, K. Tu and Z. Chen, *J. Phys. Chem. C*, 2014, **118**, 21264–21274.
19 A. O. Fumega and V. Pardo, arXiv e-prints, 2018, arXiv: 1804.07102.
20 I. A. Gospodarev, A. V. Eremenko, T. V. Ignatova, G. V. Kamarchuk, I. G. Kolobov, P. A. Minaev, E. S. Syrkin, S. B. Feodosyev, V. D. Fil, A. Soreau-Leblanc, P. Molinie and E. C. Faulques, *Low Temp. Phys.*, 2003, **29**, 151–154.
21 F. Ersan, S. Cahangirov, G. Gökoğlu, A. Rubio and E. Aktürk, *Phys. Rev. B*, 2016, **94**, 155415.
22 V. V. Mazurenko, M. V. Valentyuk, R. Stern and A. A. Tsirlin, *Phys. Rev. Lett.*, 2014, **112**, 107202.
23 G. Beutier, S. P. Collins, O. V. Dimitrova, V. E. Dmitrienko, M. I. Katsnelson, Y. O. Kvashnin, A. I. Lichtenstein, V. V. Mazurenko, A. G. A. Nisbet, E. N. Ovchinnikova and D. Pincini, *Phys. Rev. Lett.*, 2017, **119**, 167201.
24 D. Pincini, F. Fabrizi, G. Beutier, G. Nisbet, H. Elnaggar, V. E. Dmitrienko, M. I. Katsnelson, Y. O. Kvashnin, A. I. Lichtenstein, V. V. Mazurenko, E. N. Ovchinnikova, O. V. Dimitrova and S. P. Collins, *Phys. Rev. B*, 2018, **98**, 104424.
25 I. B. Bersuker, *J. Phys.: Conf. Ser.*, 2017, **833**, 012001.
26 J. P. Perdew, K. Burke and M. Ernzerhof, *Phys. Rev. Lett.*, 1996, **77**, 3865–3868.
27 G. Kresse and J. Furthmüller, *Phys. Rev. B: Condens. Matter Mater. Phys.*, 1996, **54**, 11169–11186.
28 G. Kresse and J. Hafner, *Phys. Rev. B: Condens. Matter Mater. Phys.*, 1993, **47**, 558–561.
29 E. Vatansever, S. Sarikurt and R. F. L. Evans, *Mater. Res. Express*, 2018, **5**, 046108.
30 S. Grimme, *J. Comput. Chem.*, 2004, **25**, 1463–1473.
31 F. Ersan, H. D. Ozaydin and O. Üzengi Aktürk, *Philos. Mag.*, 2019, **99**, 376–385.
32 D. Kaltsas and L. Tsetseris, *J. Phys.: Condens. Matter*, 2017, **29**, 085702.
33 J. Wilson and A. Yoffe, *Adv. Phys.*, 1969, **18**, 193–335.
34 Y. Ma, Y. Dai, M. Guo, C. Niu, Y. Zhu and B. Huang, *ACS Nano*, 2012, **6**, 1695–1701.
35 D. W. Boukhvalov, D. R. Dreyer, C. W. Bielawski and Y.-W. Son, *ChemCatChem*, 2012, **4**, 1844–1849.
36 I. V. Kashin, S. N. Andreev and V. V. Mazurenko, *J. Magn. Magn. Mater.*, 2018, **467**, 58–63.
37 A. I. Liechtenstein, M. I. Katsnelson and V. A. Gubanov, *J. Phys. F: Met. Phys.*, 1984, **14**, L125–L128.
38 G. Duvjir, B. K. Choi, I. Jang, S. Ulstrup, S. Kang, T. Thi Ly, S. Kim, Y. H. Choi, C. Jozwiak, A. Bostwick, E. Rotenberg, J.-G. Park, R. Sankar, K.-S. Kim, J. Kim and Y. J. Chang, *Nano Lett.*, 2018, **18**, 5432–5438.
39 A. Togo and I. Tanaka, *Scr. Mater.*, 2015, **108**, 1–5.
40 G. V. Kamarchuk, A. V. Khotkevich, V. M. Bagatsky, V. G. Ivanov, P. Molinié, A. Leblanc and E. Faulques, *Phys. Rev. B: Condens. Matter Mater. Phys.*, 2001, **63**, 073107.